GMS Presents:

The STaRS Program
Research Symposium

Thursday, August 11, 2016

Boston University Graduate Medical Sciences
Summer Training as Research Scholars

STaRS Research Symposium 2016

Welcome to the Annual Summer Training as Research Scholars (STaRS) Research Symposium, hosted by the Division of Graduate Medical Sciences. The students have spent this summer conducting research in labs across the BU Medical Campus and we hope you enjoy learning more about their projects.

11:00 – 11:15 am **Welcome**

Maria Ramirez, PhD
Director, STaRS Summer Research Program

Lynese Wallace
Program Administrator, STaRS Summer Research Program

11:15 – 12:30 pm **Oral Presentations**

11:15am: Denston Carey, Jr.

11:30am: Nirisha Commodore

11:45am: Logan Wolfel

12:00pm: Yuying Guo

12:15pm: Charles Laurore

12:30 pm **Lunch**

12:40 – 1:20 pm **Poster Session A**

- Marissa Baccas
- Erika Banuelos
- Kevin Delijani
- Kyle Rodrigues

1:20 – 2:00 pm **Poster Session B**

- Kathryn Odamah
- Luis Perez Valencia
- Michael Rosario

2:00 – 2:30 pm **Poster Session C**

- Chioma Anyikwa
- Joanna Ortega
- Lauren Roberts
- Celina Duran

2:30 – 3:00 pm **Presentation of Certificates & Closing Remarks**

Maria Ramirez, PhD
Director, STaRS Summer Research Program

Lynese Wallace
Program Administrator, STaRS Summer Research Program

Chioma Anyikwa
Boston University School of Medicine
Class of 2019

In Vitro Modeling of Functional Vascular Smooth Muscle Cells

Chioma Anyikwa, Francesca Seta
Vascular Biology Section, Boston University School of Medicine, Boston Medical Center, Boston, MA 02118

Background: Arterial stiffness, or loss of arterial compliance, is a risk factor for many cardiovascular diseases. The aorta and other elastic arteries may stiffen with age, obesity and other risk factors. Alterations in vascular smooth muscle (VSM) cell function have been causally linked to arterial stiffness. However, the discovery of VSM molecular mechanisms reflective of the in vivo pathogenesis, has been hampered by the fact that VSM cells change their phenotype when isolated in vitro. The goal of this project is to develop an in vitro model of VSM cells that retain the same functional properties as in vivo, in order to accurately study the effects of various treatments against arterial stiffness. It has been observed that VSM cells cultured in the presence of fetal bovine serum (FBS), a growth-stimulating factor, acquire a proliferative phenotype and lose their contractile properties. We hypothesize that VSM cells cultured in FBS-starved medium are able to regain their contractile function, compared to VSM cells cultured in FBS-containing medium.
Methods: VSM cells were isolated from aortas of mice by enzymatic digestion with collagenase and elastase, and grown in a DMEM medium containing 10% FBS and 1% antibiotics-antimycotics. Once the cells reached 90% confluency, they were split into 4 plates and grown into 4 different conditions: 10% FBS, 10% FBS on gelatin-coated plate, no FBS and no FBS on gelatin-coated plate. After 72 h, RNA was extracted from VSM cells and reverse transcribed into cDNA. Quantitative RT-PCR was performed in order to measure mRNA levels of MYH11, ACTA2 (smooth muscle actin), and myocardin, as indices of VSM contractile phenotype, and Ki67, a proliferation marker.
Results: VSM cells grown in the presence of 10% FBS and 10% FBS on gelatin-coated plates had higher levels of Ki67, and lower levels of MYH11, myocardin and smooth muscle actin, compared to cells grown without FBS.
Conclusions: When cultured in absence of FBS, VSM cells regain their contractile properties, as measured by increased levels of contractile proteins MYH11, smooth muscle actin and myocardin while decreasing proliferation, as indicated by decreased Ki67. This preliminary data indicates that we will be able to use VSM cells grown in absence of FBS as an effective in vitro model to study the role of VSM cells in arterial stiffness to discover the molecular mechanisms involved and possible therapeutic targets.

Marissa Baccas
Fayetteville State University
Class of 2017

The Effects of CK2 Inhibition on Cardiac Marker Expression in *Xenopus laevis* Embryos

Marissa Baccas, Maria Isabel Dominguez

Department of Hematology and Oncology, Boston University School of Medicine, Boston Medical Center, Boston, MA 02118

Background: The kinase CK2 is a positive component of Wnt signaling. Mouse embryos that lack *CK2α* (knockout) die in utero with uncharacterized morphological defects in the heart. We can reproduce these morphological defects in *Xenopus laevis* frog embryos by treating them with the CK2 inhibitor TBB. Here, we will use *Xenopus* embryos treated with TBB to characterize molecular defects in the heart due to lack of CK2 activity. We will analyze genes that play important roles in the formation of the heart (*Nkx2.5, Islet1, Tbx1, Tbx5* and *Mef2c*). Our hypothesis is that *Islet1* and *Tbx1* will be decreased in TBB treated *Xenopus* embryos. We expect that Islet1 will be downregulated because in β-catenin knockouts (key Wnt signaling component) Islet1 is downregulated during heart development. We expect that Tbx1 will be downregulated because the phenotype of *CK2α* knockout mice has similarities to that of *Tbx1* knockout mice. `

Methods: *Xenopus laevis* embryos were treated or not with different concentrations of the CK2 inhibitor, 4,5,6,7-tetrabromobenzotriazole (TBB), at stage 12 for 5 hours. Then TBB was washed. Embryos were photographed at different stages (12, 13-14, 20, 23-24, 28, 33-34, 37-38) to observe overall phenotype. In addition, at these stages two embryos were stopped for Reverse Transcription PCR (RT-PCR) to analyze changes in expression of the cardiac genes. At stage 46, embryos were fixed for whole-mount immunofluorescence with anti-cardiac actin to assess morphological heart defects.

Results: We set the conditions for PCR of *Nkx2.5, Islet1, Tbx1, Tbx5* and *Mef2c*. *NKx2.5* and *Islet1* were upregulated at stages 13-14 (2.5 hours post treatment) and 20 (5 hours post treatment) in a dose dependent manner. However, after the drug was washed, these genes were no longer upregulated. There was no change in the expression of Tbx1 at any stage or drug concentration.

Conclusions: CK2 inhibition in *Xenopus* leads to an increase in the expression of *Nkx2.5* and *Islet1* but has no effect on *Tbx1*. TBB needs to be present for a change in the expression of *Nkx2.5* and *Islet1* to happen. Our next steps are to repeat the experiment in frog embryos and to test whether the same genes will be affected in mouse embryos. The *Islet1* upregulation contradicts what previous studies have shown knocking out β-catenin. Therefore, in future studies we will conditionally knock out CK2α in the heart and analyze the phenotype in these mice and their differences with the β-catenin conditional knockouts.

Erika Banuelos
Brown University
Class of 2018

Inhibitory IgG Interferes with Macrophage Killing of Bacteria via the Fc-FcR pathway

Erika Banuelos, Jiyoun Kim
Department of Pathology and Laboratory Medicine, Boston University School of Medicine, Boston, MA 02118

Background: Sepsis is one of the main causes of death in hospitals around the globe. Sepsis results in a 50% mortality, demonstrating that there are vast differences in patients' response during treatment. Understanding the mechanism for clearance of bacteria can allow us to understand why some patients die and others live. Previous studies show that inhibitory IgG in plasma prevents killing of bacteria by macrophages. To further dissect the mechanism of this inhibition, we studied which component of IgG, Fab or Fc, contributes to the inhibitory response. We hypothesize that this inhibitory activity is mediated via the Fc fragment of IgG-Fc Receptor (FcR) on the surface of macrophages' pathway. This binding stimulates phagocytic cells to destroy infected cells.
Methods: A Plasma Enhanced Killing (PEK) assay was performed to determine the bacterial killing capacity of plasma from naïve ICR mice. Bacteria are collected by excising and homogenizing the cecum and quantified. Serum is incubated with bacteria at 37 C to opsonize the bacteria for 1 hr. The thioglycollate elicited macrophages were mixed with the opsonized bacteria and incubated for 1 hr. The mixture was plated on blood agar plates and incubated at 37C in aerobic and anaerobic condition for 20 hrs and the number of residual bacteria was determined by counting CFU (colony forming unit). Based on this number each plasma was categorized into high and low PEK, with a higher PEK indicating better bacterial killing. IgG was purified from pooled serum and analyzed for killing capacity changes along with the rest of the serum (IgG depleted). The level of IgG and IgM were quantified by ELISA.
Results: The assay for bacterial killing for 40 plasma includes macrophages, bacteria and plasma, and showed a wide range in the ability to enhance/inhibit killing capacity as shown in previous studies. Depletion of inhibitory IgG from pooled plasma from the low PEK group shows higher number of bacteria, i.e., lower killing compared to purified IgG in PEK assay, which is somewhat distant from our anticipated result as depletion of inhibitory IgG should increase bacterial killing capacity. To clarify these unanticipated result, we quantified the levels of IgM and IgG in the intact, IgG depleted, and purified IgG, and found that significant level of IgG present in IgG depleted plasma. Our high and low PEK assays contained 22.6% intact IgG and 53.2% intact IgG, respectively.
Conclusions: Bacterial killing capacity of plasma varies among naïve ICR mice. Inhibitory IgG in non-killing plasma might prevent killing of bacteria, leading to less clearance of bacteria. While a substantial portion of IgG is depleted in plasma, it is not complete and could be the potential source of the unanticipated results in the PEK assay. Further studies are anticipated to complete depletion of IgG and separation of Fc/Fab to further analyze the reduced bacterial killing capacity elicited by macrophage.

Denston Carey, Jr.
West Chester University of Pennsylvania
Class of 2017

Thalamic Inputs onto Neurons Derived from Distinct Progenitors in Layer 4 of the Mouse Barrel Cortex

Denston Carey, Jr., Teresa Guillamon-Vivancos, Jennifer Luebke, Maria Medalla
Department of Anatomy and Neurobiology, Boston University School of Medicine, Boston, MA

Background: Neuronal diversity underlies the brain's astounding computational ability; however, the mechanisms by which this diversity is generated are poorly understood. Neuronal precursor cells, such as radial glial cells (RGCs), and intermediate progenitor cells (IPCs) are now known to produce neurons, which can be classified into two lineages (Tbr2+ and Tbr2-) that differ morphologically and physiologically. In this study, we conduct a comprehensive investigation on differential thalamic inputs to neurons of these two lineages in layer 4 of the mouse barrel cortex. Since neurons derived from these two lineages have been shown to exhibit distinct electrophysiological and structural characteristics, it is hypothesized that thalamic interactions among them will be different as well.

Methods: This project examined neurons from Tbr2+ (n=3) and Tbr2- (n=3) lineages in layer 4 of the mouse barrel cortex. Intracellularly filled neurons were immunostained for the vesicular glutamate transporter 2 (VGLUT2), a marker of thalamic excitatory inputs, and imaged at high resolution using confocal microscopy. Neurolucida 360 software was used to reconstruct representative dendrites and the soma, and to quantify spines and VGLUT2+ thalamic appositions on filled neurons. Several analyses were performed to assess relative spine density, spine morphology, and distribution across the dendritic arbor, as well as density and distribution of thalamic appositions. Statistical analyses were performed with a two-tailed Students t-test, differences with a p-value less than 0.05 were considered significant.

Results: There were no differences in total apposition density among lineages (density ± SEM, Tbr2- lineage = .70 ± .1 μm^{-1}; Tbr2+ lineage = .50 ± .1 μm^{-1}, p = .30). Neurons of the Tbr2- lineage exhibited a trend of both a higher mushroom spine proportion relative to total spines (mean percentage ± SEM, Tbr2- lineage = 12 ± 2 %; Tbr2+ lineage = 8 ± 1 %, p = .077) as well as mushroom spine density (mean density ± SEM, Tbr2- lineage = .16μm^{-1} ± .02 μm^{-1}; Tbr2+ lineage = .11 μm^{-1} ± .02 μm^{-1}, p = .14) and mushroom head apposition density (density ± SEM, Tbr2- lineage = .09 ± .02 μm^{-1}; Tbr2+ lineage = .04 ± .02 μm^{-1}, p = .14). There was also a trend towards greater soma apposition count in Tbr2- neurons (count ± SEM, Tbr2- lineage = 39 ± 9 appositions; Tbr2+ lineage = 11 ± 6 appositions, p = .059). Lastly, it was noted that the proportion of branched spines that were apposed relative to total branched spines was trending towards being greater in the Tbr2- lineage (percentage ± SEM, Tbr2- lineage = 9 ± 2 %; Tbr2+ lineage = 4 ± 2 %, p = .16).

Conclusion: Though there were no significant differences brought to light in this study, the absence of differences as well as the trends found, provided insight in regards to the similar thalamic interactions and spine characteristics that these lineages were found to have. The absence of differential input suggests that thalamic input onto these two lineages in layer 4 of the mouse barrel cortex is similar, and not affected by their differing neuronal lineages. The trends found here also suggest that mushroom spines play a prominent role in Tbr2- lineage neuron's interactions with the thalamus.

Nirisha Commodore
University of the Virgin Islands
Class of 2018

Identification of Aryl Hydrocarbon Receptor Antagonists with Biological Activity *In Vitro*

Nirisha Commodore, Alejandra Ramirez-Cardenas, David Sherr, PhD

Boston University School of Public Health, Boston University School of Medicine, 72 East Concord St. Boston, MA 02118

Background: There are 85,000 anthropogenic chemicals registered by the EPA, of which relatively few have been evaluated for their effects on human health. The Aryl Hydrocarbon Receptor (AHR) is a ligand-activated transcription factor that is notorious for its role in mediating the effects of environmental pollutants in several physiological and pathophysiological processes, for example, cancer. Many pollutants have been identified as AHR agonists. However, few antagonists have been detected. Therefore, a library of compounds was virtually screened to identify new compounds that displayed similar binding to the AHR as the known AHR antagonist, 2-((2-(5-bromofuran-2-yl)-4-oxo-4H-chromen-3-yl) oxy) acetamide (CB7993113). Five compounds, denoted as NEU1-5, were recognized as potential antagonists based on their similarity to CB7993113 and their predicted ability to bind the AHR.
Methods: To test the functional characteristics of these compounds, AHR-driven reporter assays using a murine hepatoma cell line (H1G1) and an immortalized human epithelial breast cell line (MCF10F) were employed to assess the NEU compounds' ability to inhibit AHR activation. Titrations of a non-toxic AHR agonist, Beta-naphthoflavone (BNF), were performed to determine a concentration at which the activation of the AHR would be optimal for detecting any inhibition caused by the NEU compounds. Toxicity of compounds was determined by quantification of cell metabolic activity at various time points following cell treatments (MTT assay).
Results: Of the five compounds tested for AHR inhibition, NEU4 showed the most promising results. At concentrations of 10 and 50 uM, percent inhibition of AHR activation in NEU4-treated cells was significantly higher than the cells treated with 2.5 uM BNF (p-values, 0.00231, 0.00435 respectively). Toxicity quantification confirmed that there was no significant change in percent viability of cells following treatments.
Conclusion: These experiments suggest that NEU4 may be a potent antagonist of the AHR and may represent a novel targeted cancer therapeutic.

Kevin Delijani
Emory University
Class of 2018

Symbiotic Relationship in Combining Adjuvants

Kevin Delijani, Christina Lisk, Michael Reiser, Lee Wetzler

Boston University Medical Center, Department of Medicine, Section of Infectious Diseases

Adjuvants play an integral role in vaccines as it enhances the inflammatory response; however, the mechanism is not well known. A complete understanding of how adjuvants stimulate an inflammatory response would allow for more efficient vaccine composition. Therefore, investigating the mechanism of different toll like receptors (TLRs) and their interact is crucial. Multiple adjuvants may enhance the inflammatory response via an upregulation of signaling molecules, cytokines and interferons. In this study, we tested the activation response of bone marrow-derived dendritic cells (BMDCs) stimulated with different TLR adjuvants individually or in combination. ELISAs were utilized to measure activation. Our hypothesis is BMDCs stimulated with two TLR adjuvants signaling through different pathways will have the greatest response.

Bone marrows cells were isolated and differentiated into BMDCs successfully from C57BL/6 mice following previously published protocols. Cells were plated in a 6-well plate at $2x10^6$ cells/ plate. Concentrations for adjuvants were determined based on previous studies within the lab. Cells were incubated with PorB, Poly(I:C), or both for 6 hours. Non-immunogenic antigen, ovalbumin (OVA), was used in all adjuvant stimulations. PBS was the negative control. ELISAs were utilized to determine the concentration of TNF α, IL-6, and IFN β.

Stimulation with multiple adjuvants gave the greatest response in all endpoints tested for. Poly(I:C) and PorB had a significant increase over PorB or Poly(I:C) alone in IL-6, TNF α, and IFN β. Furthermore, PorB had a greater response of each cytokine and interferon than Poly(I:C).

The results support our hypothesis that signaling through different TLR adjuvants can lead to a higher activation response of BMDCs as measured by pro-inflammatory cytokines and interferon expression. We showed that the concentration of IL6 and TNF α was statistically significant greater when BMDCs were stimulated with multiple adjuvants. Interestingly, synergy is shown between PorB and poly(I:C) for IL-6 and TNF α. The adjuvants chosen signal through different intracellular pathways. This suggests that activation of a combination of TLR pathways leads to increased pro-inflammatory cytokines – IL6 and TNF α. The increase in cytokine concentration may be influential to upregulate antibody production. Both IL-6 and TNF α stimulate B Cells that can create protection against bacteria. Poly(I:C) is an intracellular TLR3 agonist therefore the increase in IFN β expression was expected for poly(I:C) alone. The addition of PorB, however, showed a further increase of IFN β. The results of this study highlight how mechanistically targeting TLR receptors can influence BMDC cytokine and interferon expression. Mechanistic studies such as this are greatly needed to fully understand the immune system interactions and provide better vaccines.

Celina Duran
Boston University School of Medicine
Class of 2019

Optimizing smoking cessation interventions within Low Dose CT screening: A Systematic Review

Celina Duran, Jonathan Iaccarino, Hasmeena Kathuria

Background: The National Lung Screening Trial (NLST) showed a 20% reduction in lung cancer mortality with low dose CT (LDCT) screening in high risk individuals with a significant smoking history. Smoking cessation interventions are now a Center for Medicare and Medicare Services requirement to receive coverage for LDCT screening. However, the optimal approach for delivering cessation interventions in the LDCT screening context is currently unknown.

Methods: We performed a systematic review to assess the ideal timing, intensity, and type of intervention for smoking cessation in patients undergoing LDCT with a primary outcome of 6-month smoking abstinence and secondary outcomes of change in readiness to quit and cost effectiveness. We searched for studies in which adults undergoing LDCT screening underwent a smoking cessation intervention using the following databases: MEDLINE, the Cochrane Library, Web of Science, EMBASE, and PsycINFO. Of 2212 identified studies, 8 studies met inclusion criteria. Two reviewers independently reviewed each study to assess eligibility and extracted information using pre-specified protocol for included studies.

Results: We identified 8 studies that evaluated smoking cessation counseling within the LDCT setting. Two trials evaluated the efficacy of quit rates with self-help materials, with no apparent improvement in our primary and secondary outcomes. Five studies compared clinician-delivered counseling to less intensive intervention, each using different smoking cessation techniques. While the cessation technique differed among studies, more intensive cessation counseling appeared to have greater improvement in 6-month smoking abstinence and readiness to quit. One study found higher 6-month smoking abstinence when cessation counseling was performed before LDCT compared to after screening. A final study addressed the cost-effectiveness of counseling as compared to counseling and pharmacologic cessation aids and found the addition of pharmacotherapy significantly increased cost-effectiveness. We identified no studies evaluating the utility of e-cigarettes or other novel approaches for smoking cessation in the context of LDCT screening.

Conclusions: Providing smoking cessation treatment in conjunction with annual lung cancer screening offers the unprecedented opportunity to dramatically reduce smoking related morbidity and mortality. We identified gaps in knowledge about smoking cessation interventions regarding the optimal intervention, timing of delivery, and pharmacotherapy approaches when applied to the LDCT setting. Self-help materials offer minimal, if any, benefit within LDCT programs. Conversely, clinician-delivered counseling may improve smoking cessation quit rates. Research on innovative approaches to achieve sustained abstinence in these older, heavily addicted screened patient is warranted.

Yuying Guo
Bryn Mawr College
Class of 2018

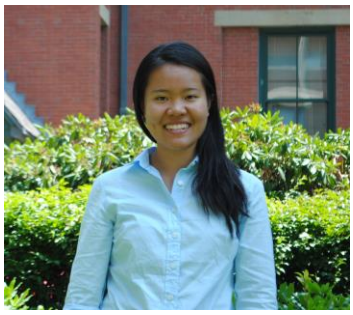

Real-time portable viral genome sequencing

Yuying Guo, Emily Speranza, John H. Connor

National Emerging Infectious Diseases Laboratories, Boston University School of Medicine, Boston, MA 02118

Monitoring and observing infectious disease outbreaks, such as the 2014 Ebola virus outbreak, is contingent on accessible and efficient viral genome sequencing. To better understand how viruses are evolving during outbreaks, such as developing mutations that will enable them to spread more efficiently from host to host or to elicit more virulence, real-time genome sequencing is essential. But in areas of such outbreaks, resources are limited and local sequencing facilities are nonexistent. Therefore sequencing devices must be brought to point-of-care areas during outbreaks. One option is to use a nanopore-based sequencer, which is a *portable* sequencing device that produces real-time sequencing, and conveniently connects to a computer through a USB port. The goal of this project is to establish the use of nanopore sequencing for two viruses responsible for the recent global health concerns, the Ebola virus and Zika virus. To sequence these viruses, RT-PCR strategies were used to create double-stranded DNA fragments from non-infectious virus samples. These DNA fragments were then assembled into a sequencing "library" and sequenced using nanopore technology. The MinION, the nanopore sequencer, generated 1,387 unique reads of lengths ranging from 1,000 to 2,500 base pairs in a 3-hour sequencing run. When compared to a reference genome, full coverage at a depth of 90X redundancy was achieved. The MinION generated a sequenced genome that is in agreement with the genome generated by RNA-seq, demonstrating its ability to generate accurate reads in a short, feasible amount of time, which is critical for its use on the grounds of an infectious disease outbreak. Single nucleotide variant (SNV) calling was performed on the sequenced Ebola genome to identify mutations within the genome. Among the 17 SNVs identified, 2 were transversion mutations and 15 were transition mutations. We are now testing the feasibility of this approach for sequencing Zika virus. Nanopore technology has allowed for real-time sequencing of the Ebola virus genome, and has generated a reliable sequenced genome.

Chinaemere Igwebuike
Boston University School of Medicine
Class of 2020

Nucleophosmin Oligomerization Associated with Susceptibility to Ischemia-Induced Acute Kidney Injury In-Vitro

Chinaemere Igwebuike, Zhiyong Wang and Steven C. Borkan

Department of Nephrology, Boston University School of Medicine, Boston Medical Centre, Boston MA 02118

Background: Improved understanding of renal cell death in acute kidney injury has produced new and specific targets for clinical intervention. Nucleophosmin (NPM1), a nucleolar phosphoprotein whose oligomerization prevents cell injury, may be a novel target in the prevention of acute kidney injury.

Methods: Primary renal epithelial cells, a major target of kidney injury, were exposed to transient ATP depletion in a dosage capable of inducing epithelial cell apoptosis and decreased cell survival. Cells were treated with NSC348884, a drug that monomerizes NPM1, and geranylgeranylacetone, a drug that ameliorates ischemic acute kidney injury, for 24 hours prior to ATP depletion. Cell viability was measured using propidium iodide staining and computerized image cytometry. The oligomeric NPM1 protein was measured against its cytotoxic, monomeric form using SDS-PAGE and native Western blotting.

Results: Cell viability analysis shows increased cell death in cell treated with NSC348884, drug that promotes monomerization of NPM1. In contrast, cells treated with geranylgeranylacetone, drug that improves damage caused by ischemia-induced AKI, showed a slight increase in cell viability. Western blot analysis shows large amounts of the protective oligomeric NPM1 in control and GGA-treated cells, but less oligomeric NPM1 in NSC348884-treated cells.

Conclusion: Nucleophosmin is a nucleolar phosphoprotein that acts as a chaperone to Bax in the apoptotic cascade. Although nucleophosmin is found primarily in the nucleolus, it has been documented that metabolic stress can cause nucleophosmin to translocate to the cytosol and possibly undergo changes in oligomerization. NSC348884, a drug that promotes NPM1 monomerization, has been shown to decrease oligomeric NPM1 and decrease cell viability. In contrast, geranylgeranylacetone, a drug that protects against ischemic kidney injury, is shown to ameliorate this stress-associated decrease in NPM oligomers and prevent cell death. These data support the hypothesis that altering NPM1 oligomerization may be a feasible strategy in preventing ischemia-induced acute kidney injury.

Jabari Jackson
Tougaloo College
Class of 2018

Role of Albumin in Proximal Tubule Mitophagy

Jabari Jackson, Ryan Mulhern, Chino Igwebuike, Andrea Havasi, MD

Background: The kidneys extract waste from blood, balance body fluids, form urine, and aid in other important functions of the body. The primary unit of kidney is the nephron (see image). In proteinuric kidney diseases the glomerulus is damaged resulting in large amount of albumin leaking into the proximal tubule, the segment after the glomerulus. The proximal tubule is responsible for reabsorption of this albumin. Autophagy is a self-degradative process that balances sources of energy during starvation and stress and also plays a housekeeping role in removing misfolded or aggregated proteins and damaged organelles. Mitophagy is the selective degradation of mitochondria by autophagy. It often occurs to defective mitochondria following damage or stress.

Methods: The proximal tubules reabsorb large amount of albumin in nephrotic kidney diseases. In our previous experiments we showed that albumin reabsorption inhibits autophagy in the proximal tubular cells. The proximal tubules have high energy requirements and they are rich in mitochondria. We tested the hypothesis if albumin endocytosis inhibits mitophagy. To test our hypothesis we treated primary proximal tubule cells harvested from renal cortexes of mice with albumin and measured mitophagy.

Results: As a result of albumin treatment to the proximal tubule cells, more mitochondrion had mitophagy. The treatment of albumin when compared to the cells without treatment indicates that mitophagy is occurring. From prior research we conclude that mitophagy is also inhibited increasing cell toxicity.

Conclusion: Albumin inhibits mitophagy in cultured primary proximal tubular cells and might lead to cell toxicity.

Charles Laurore
Williams College
Class of 2018

Developing an Adipose Tissue Fibrosis Model

Charles Laurore, Michael Jager, Matthew D. Layne

Department of Biochemistry, Boston University School of Medicine, Boston, MA 02118

Background: The deposition and remodeling of extracellular matrix (ECM) or fibrosis in adipose tissue is emerging as a contributor to metabolic disease. Various stress factors including inflammation and hypoxia can result in adipocyte death and apoptosis. What is currently unknown is the type of cells that are responsible for the deposition of ECM as well as the means by which this process is regulated. The goal of our study is to establish a novel adipose tissue fibrosis explant model to characterize the mechanism of fibrosis in adipose tissue.

Methods: Epididymal adipose tissue explants were isolated from male mice, placed in medium, treated with transforming growth factor β (TGFβ, a pro-fibrotic cytokine) to induce fibrosis, fixed with zinc formalin, processed into paraffin blocks, cut into 5 μm sections using a microtome, and fixed onto microscope slides. These tissue sections were then analyzed using picrosirius red staining for collagen (and assessed using polarized light microscopy), and immunofluorescence microscopy. Epididymal adipose tissue explant proteins were analyzed by Western blot to identify fibrotic and myofibroblast markers (aortic carboxypeptidase-like protein, smooth muscle α actin (α-SMA), and collagen (ColI) and adipocyte markers (fatty acid binding protein (FABP4) and perilipin).

Results: Compared with controls, Western blot analysis indicated an increase in α-SMA in the TGFβ treated epididymal adipose tissue explants both 2 and 4 days following treatment. An increase in perilipin in TGFβ treated epididymal adipose tissue explants was also observed. Immunofluorescent staining for α-SMA indicated patchy areas of myofibroblast accumulation. Picrosirius red staining for collagen also defined areas of fibrosis (pericellular and perivascular).

Conclusions: Our studies established a simplified explant model of adipose tissue fibrosis and identified fibrotic changes surrounding both the blood vessels and around the adipocytes themselves. The increase in perilipin in TGFβ treated epididymal adipose tissue explants could indicate an increase in adipocyte size (hypertrophy) and/or number (hyperplasia). The increase in α-SMA in the TGFβ-treated epididymal adipose tissue explants likely indicates changes in myofibroblasts. Ongoing work using this model will hopefully identify the cells responsible for collagen production in adipose tissue fibrosis.

Kathryn Odamah
Duke University
Class of 2017

CX-4945: A Proposed Treatment for High-Risk Neuroblastoma

Kathryn Odamah, Haiwei Lian, Hui Feng

Department of Pharmacology & Experimental Therapeutics
Boston University School of Medicine, Boston Medical Center, Boston, MA 02118

Background: Neuroblastoma is a distressing childhood cancer of the nervous tissue, most commonly formed in the adrenal gland. Increased MYCN expression has been found in 30% of neuroblastomas, and aberrant activity of protein kinase *CK2* is found in MYCN-driven neuroblastomas at advanced stages, suggesting that MYCN and *CK2* may act together in neuroblastoma pathogenesis. CX-4945 is a potent, selective ATP inhibitor of *CK2*. We wanted to determine the role of *CK2* in MYCN-driven neuroblastoma pathogenesis and assess the efficacy of CX-4945 in treating human MYCN-driven neuroblastoma.
Methods: To determine the *in vitro* effects of *CK2* inhibition, RNAi knockdown and CX-4945 treatments were used to inactivate *CK2* in multiple human neuroblastoma cell lines with or without MYCN amplification. I independently transfected the two short hairpin RNAs that were used to knockdown the *CK2*α gene in these cell lines. Cell viability assays were used to determine the proliferative status of each cell line. To determine the role of *CK2* in neuroblastoma formation *in vivo*, *CK2*α knockout zebrafish were previously generated in our lab using CRISPR-CAS technology. Heterozygous *CK2*α knockout fish were isolated and bred to *d*β*h-MYCN;d*β*h-EGFP* transgenic fish. We are currently monitoring the offspring and are in the process of determining the effects of *CK2*α genetic loss on the onset and progression of MYCN-driven neuroblastoma.
Results: We have obtained preliminary data to support our hypothesis. Statistical analyses showed that *CK2* enzymatic subunit expression was upregulated in human neuroblastoma patient samples with MYCN amplification. Western blot analyses showed that MYCN protein levels were decreased in human neuroblastoma cell lines with MYCN amplification following treatment with CX-4945. MYCN protein levels began to decline by 8 hours and were undetectable by 12 hours. Cell viability was decreased in all neuroblastoma cell lines with MYCN amplification, as well as in all non-MYCN neuroblastoma cell lines following treatment with CX-4945.
Conclusions: Our findings show that *CK2* expression is significantly correlated with human neuroblastoma samples with MYCN amplification. We also show that CX-4945 treatment is effective in decreasing MYCN protein levels and significantly reducing viability of human neuroblastoma cell lines. Future work will assess: a) the effects of genetic inactivation of *CK2* on neuroblastoma cell growth and survival as well as on tumor development, and b) the ability of CX-4945 to promote neuroblastoma tumor regression in zebrafish and preclinical murine models. Results from such further research will enable the advancement of CX-4945 into neuroblastoma clinical trials.

Joanna Ortega
Boston University School of Medicine
Class of 2019

Optimization Of AAT Antibody Staining In 293 Cell Lines Transduced with AAT For Downstream Use In AATD hiPSC-Hepatic Cells

Joanna Ortega, Joseph Kaserman, Andrew Wilson

Center for Regenerative Medicine, Boston University School of Medicine, Boston Medical Center, Boston MA 02118

Background: Alpha-1 antitrypsin deficiency (AATD) is an important autosomal co-dominant genetic disorder thought to affect 1 in 2000 individuals and results in both lung and liver disease. There are currently 120 documented mutations with the most common, known as the "Z mutation, resulting from a single base pair change causing a Glu342Lys amino acid substitution. This results in a conformational change leading to misfolding and polymerization of the mutated protein. The polymerized protein accumulates within the ER of hepatocytes, predisposing individuals to liver disease. Previous antibodies identified the alpha-1 antitrypsin protein without distinction between the Z polymer (ZAAT) and the wild type protein (MAAT). Two novel monoclonal antibodies, 2C1 and PiZmAb, were recently developed to identify the Z mutant polymer variant. Our project aim was to generate 3 working assays for 2C1 and PiZmAb in 293 cell lines expressing AAT for future use in AATD CRISPR corrected hIPSC-hepatic cell syngeneic clones previously generated by our lab.

Methods: Differences in intracellular and extracellular protein within 293 cells transduced with a lentivirus to express MAAT-GFP and ZAAT-GFP were analyzed by intracellular flow cytometry, ELISA, and immunostaining. For each assay the specificity of 2C1 and PiZmAb was compared to a pan-alpha -1 antibody.

Results: Intracellular AAT protein was quantified by intracellular flow cytometry on fixed permeabilized 293 ZAAT and MAAT lines using mean fluorescent intensities (MFIs). Results for each antibody from the 293 ZAAT and MAAT lines respectively were: AAT antibody 133 and 22.1; 2C1 antibody 85 and 24.6; and PiZmAb 3.89 and 4.14. A working ELISA was not obtained for either 2C1 or PiZmAb. Immunostaining with 2C1 and PiZmAb demonstrated more specific binding for ZAAT as compared to the pan-alpha-1 antibody.

Conclusions: 293 cells transduced to express ZAAT showed the expected intracellular protein accumulation as compared to MAAT expressing cells. However, the 2C1 antibody did not demonstrate specificity for ZAAT as compared to MAAT in 293 cell lines when used in intracellular flow cytometry. Immunostaining with 2C1 and PiZmAb indicated a higher amount of intracellular accumulations for 293 ZAAT cells in comparison to 293 MAAT cells. Finally the PiZmAb requires further optimization prior to its use in hIPSC-hepatic cells.

Luis Perez Valencia
Connecticut College
Class of 2017

Lymphocyte isolation from lamina propria and lymph nodes in a murine model of Shiga toxin producing *E.coli* infection

Luis J. Perez Valencia, Greg Hall, Shinichiro Kurosawa, Deborah J. Stearns-Kurosawa

Department of Pathology and Laboratory Medicine, Division of Graduate Medical Sciences, Boston University School of Medicine, Boston MA 02118

Background: Shiga toxin-producing *Escherichia coli* (STEC) is a common food-borne intestinal pathogen which can lead to a life threatening complication called hemolytic uremic syndrome with toxin-induced kidney and neurologic injury. This study explores mucosal lymphocyte dynamics during STEC infection which are not currently known. Colitis and dysbiosis induced by oral dextran sodium sulphate (DSS) allows for murine STEC infection and provides an animal model for isolation of intestinal and regional lymph node lymphocytes. Methods were developed to isolate viable immune cells from lamina propria and mesenteric lymph nodes of DSS +/- STEC mice, identify major immune cell populations, and test their ability to be activated.

Methods: Female C57BL/6 mice were given sterile 2.5% (w/v) DSS in drinking water for 5 days. On the 5^{th} day, mice were orally gavaged with 7 x 10^7 CFU STEC strain TW14589. Six to seven days after gavage, the descending colon and mesenteric lymph nodes were harvested for lymphocyte isolation. It was critical to the viability of cells to maintain the tissues on ice before incubations. Isolating cells from colons (2 cm – 4 cm) consisted of meticulous removal of fat and cutting the tissues into 1 cm pieces followed by incubations in HBSS containing 5 mM EDTA and 1 mM DTT. Tissues were cut into 1 mm pieces to facilitate enhanced enzyme digestion with incubations in a solution of DNase, dispase, and collagenase then passing the tissues through cell strainers for further selective extraction of lamina propria mononuclear cells (LPMCs) using a Percoll gradient. Lymphocytes from lymph nodes were isolated by passing them through a cell strainer with RPMI media and subsequent centrifugation. Cell viability was determined using Trypan Blue. Cells were fixed using 4 % paraformaldehyde in PBS and permeabilized. Cells were stained with antibodies against CD4, IL-17, and IFNγ. Cell stimulation for lymph node samples were conducted by incubating at 37°C in BD GolgiStop and eBioScience Cell Stimulation Cocktail for 4 hours. Flow cytometry was conducted using BD FACSCalibur.

Results: LPMCs yields from murine colons with DSS and DSS+STEC were on average 2.68 x 10^6 cells/colon and 4.34 x 10^6 cells/colon respectively with similar yields for mesenteric lymph nodes. Cell viability after isolation was approximately 75%. LPMC isolation ranged from 6-7 hours depending on the number of samples and the protocol should be completed in one day to maintain cell viability. Staining of lymph node samples indicated $CD4^+$ cells with increased IL-17 in STEC samples.

Conclusions: The described protocol was successful in isolating viable lymphocytes in numbers sufficient for use in further assays. These preliminary findings can help to show what the immune response should look like in a STEC infection and this pilot study is the first step in protocol development for a future standardized STEC mouse model.

Tyler Pluchino
SUNY Upstate Medical University
Class of 2019

Predictors of Hospitalizations in Elderly African-American Patients with Heart Failure with Preserved Ejection Fraction

Tyler A. Pluchino[1], Marios Arvanitis[2], Frederick L. Ruberg[2]

[1]State University of New York Upstate Medical University, Syracuse, NY
[2]Boston University School of Medicine, Boston, MA

Introduction: Heart failure with preserved ejection fraction (HFpEF), is a common condition that affects approximately 1.1-5.5% of the general population and is associated with high in-hospital, short term and long term mortality which significantly increases with age. In addition, patients diagnosed with HFpEF contribute to significant costs of care. Although highly underrepresented in most studies of HFpEF, African-Americans appear to experience heart failure at an earlier age, and have more hospitalizations than people of different ethnicity. Identifying the epidemiology of HFpEF in this population is pertinent both to patients and to the healthcare industry, in order to create better therapies and reduce costs. The goal of the present study is to highlight the clinical, biochemical and echocardiographic characteristics of the disease and to identify predictors of short term hospitalization in elderly African American individuals with HFpEF.

Methods: This is a retrospective study conducted in a subset of patients from a registry of elderly African American individuals with heart failure and cardiac hypertrophy. Inclusion criteria for the registry were age ≥65, African-American race, an ICD9/10 diagnosis of heart failure and cardiac hypertrophy defined as an interventricular septal diameter ≥12mm based on echocardiogram. Patients were selected from the registry based on the absence of TTR cardiac amyloidosis and a left ventricular ejection fraction ≥45%. Differences between continuous variables were calculated using the Wilcoxon signed rank test, while the chi-squared test was used for categorical variables. The Cox proportional hazards model was used to identify predictors of 90-day hospitalization.

Results**:** Forty patients were included in our study, of whom 22 were males. Several gender-based differences were identified in our population. African-American women were found to have higher ejection fractions compared to their male counterparts (66% vs 61%, p = 0.02). Echocardiographic data also showed that men have higher left ventricular end-diastolic dimensions (47mm vs 44mm, p = 0.005) and left ventricular end-systolic dimensions (32mm vs 26mm, p = 0.004) compared to women. Creatinine (2.1 mg/dl vs 1.5 mg/dl, p=0.05) and Troponin I (0.28 ng/ml vs 0.02 ng/ml, p=0.006) were higher in the male cohort however the Troponin I levels were no longer significant after adjusting for renal function. Importantly, retinol-binding protein 4 (RBP4) (HR 1.02, p=0.02), and creatinine levels (HR 1.32, p=0.04) were associated with a 90-day hospitalization while higher hemoglobin A1C levels demonstrated a non-significant trend (HR 1.14, p=0.06).

Conclusions: Our data suggests higher RBP4 and creatinine levels are associated with short term hospital admissions in elderly African-American patients with HFpEF. The study conducted on this cohort also showed that there are differences between males and females with respect to heart size and function.

Lauren Roberts
Boston University School of Medicine
Class of 2019

Evaluation of Risks for Peripheral Bypass Surgery Readmissions and ER Visits

Lauren Roberts, Jeffrey Siracuse, Bri Krafcik, Sevan Komshian, Kimberly Lu

Division of Vascular and Endovascular Surgery, Boston University School of Medicine, Boston Medical Center, Boston, MA 02118

Background: Peripheral bypass surgery patients have very high rates of readmissions. We wanted to analyze which symptoms and comorbidities have the highest risk of readmissions or emergency visits. This information can help identify potentially resource intensive patients. This would allow physicians to heighten follow-up care with identified patients, ultimately leading to reduced post-operative complications and health institution costs.

Methods: A retrospective review and analysis of Boston Medical Center's emergency visits and readmissions of patients who received lower extremity peripheral bypass surgery was conducted. All BMC lower extremity peripheral bypass surgeries from 2007 to 2016 were included.

Results: Out of 385 discharges, there were 106 patients with an ER visit within 30 days (27.53%), 149 patients with an ER visit within 90 days (38.7%), and 227 patients with an ER visit within one year (58.86%). Of these 385 discharges, 115 patients had a readmission within 30 days (29.87%), 191 patients had a readmission within 90 days (49.61%), and 275 patients had a readmission within one year (71.43%). The patients were Caucasian (46%) and African-American (39%) males (63%) with an average age of 65. The most common comorbidities and symptoms were hypertension (86.75%), former smoker (73.25%), diabetes (58.96%), and tissue loss (54.55%). The bypass surgeries were of femoral origin (86.23%), and had popliteal targets (51.43%) and tibial targets (48.32%). The greatest indicators of the first ER visit within 90 days were hypertension (OR, 3.7) African-American race (OR, 3.03), prosthetic or cryovein anastomosis (OR, 2.14), and impaired ambulatory status (OR, 2.03). The greatest indicators of the first ER visit within one year were hypertension (OR, 4.39), African-American race (OR, 2.42) impaired ambulatory status (OR, 1.80), and prosthetic or cryovein anastomosis (OR, 1.78). Reasons for the first ER visit within one year included surgical site infection (33%), foot or leg wound (15%), graft complication (8%), and other infection (8%). The greatest indicators of having the first readmission within 90 days were dialysis (OR, 2.24), renal failure (OR, 2.07), diabetes (OR 1.78), and impaired ambulatory status (OR, 1.74). The greatest indicators of having the first readmission within one year were COPD (OR, 2.67), Medicare insurance (OR, 2.38), dialysis (OR, 2.21), impaired ambulatory status (OR, 1.97), and renal failure (OR, 1.97). Reasons for the first readmission with one year included surgical site infection (23%), graft complication (13%), foot or leg wound (12%), and problem with other leg (10%).

Conclusions: High-risk comorbidities and preoperative symptoms for ER visits and readmissions were identified. This information can be used to better treat and follow-up with high-risk patients post-operatively, while also reducing health institution costs.

Kyle Rodrigues
University of Massachusetts, Amherst
Class of 2018

Afferent renal nerve activity and brain activation in response to acute volume expansion and the impact of high salt intake on ex-vivo renal mechanoreceptor activation in Sprague Dawley rats

Kyle Rodrigues, Lillian Whelan, Alissa Frame, Richard Wainford

Pharmacology and Experimental Therapeutics, Whitaker Cardiovascular Institute, Boston University School of Medicine, Boston, MA 02118

Background: 1 in 3 adults in the US are affected by hypertension (HTN). HTN can lead to cardiovascular disease, stroke, and kidney failure. The mechanism by which the reno-renal reflex operates to manage HTN is largely unknown. Specifically, the renal afferent nerves inhibit efferent renal nerve activity by activating inhibitory neurons in the paraventricular nucleus (PVN) of the hypothalamus to cause natriuresis and normotension. The role of the afferent renal nerves in response to acute volume challenge and the impact of alpha-adrenoceptor systems in these responses are of interest.

Methods: Conscious young (3 month old) Sprague Dawley (SD) rats fed a normal 0.6% salt diet for life, post sham (S) or afferent renal nerve ablation (Renal-CAP, capsaicin 33 mM) underwent IV volume expansion (VE; 5% BW) and heart rate (HR), mean arterial pressure (MAP), urine output, and PVN neuronal activation (c-Fos expression) were determined (N=4/gp). Separate, young SD rats were fed a normal 0.6% salt (NS) or high 4% salt (HS) diet for three days. Afferent renal nerve activity was measured as substance P (SP) release in a renal pelvis assay (N=4/group). During baseline, one renal pelvis of a kidney from each rat was kept in HEPES while the other was placed in HEPES and an α-1 (prazosin, 5uM) antagonist, and the supernatant was collected.

Results: Renal-CAP attenuated the natriuretic and PVN parvocellular responses to IV VE (peak UNaV [µeq/min]; S 43±4 vs Renal-CAP 26±6, $P<0.05$, PVN Medial Parvocellular neuronal activation [c-fos positive cells]; S 49±6 vs Renal-CAP 22±5 $P<0.05$) and evoked increased MAP (MAP 90min post-VE [mmHg] S 118±3 vs Renal-CAP 132±4, $P<0.05$). In young SD rats, there was no observable difference in baseline renal pelvic (control) SP release between NS and HS diets ([pg/min]; NS 53±6 vs HS 49±4). There was also no observable difference in baseline SP release between NS and HS diets in renal pelvic treated with prazosin ([pg/min]; NS 47±4 vs HS 50±5).

Conclusions: The afferent renal nerves are critical in modulating natriuresis and normotension. In response to acute salt challenge, the afferent renal nerves activate neurons in the PVN to inhibit efferent renal nerve activity and sodium reabsorption. Blocking afferent renal nerve activity via renal-CAP during volume expansion reduces salt secretion and PVN activity in response to acute volume expansion because the afferent renal nerves are unable to provoke sympathoinhibition. Although increased MAP is an acute response to renal-CAP, it is speculated that chronic hypertension could be a result of sustained blocking of afferent renal nerve activity. Our data suggests prazosin, an α-1 antagonist, has no effect on baseline SP release. This indicates that α-1 receptors in the kidney do not play a significant role in basal afferent renal nerve activity.

Michael Rosario
University of Virgin Islands
Class of 2017

Cardiovascular Fitness is Positively Correlated with Left Entorhinal Cortical Thickness in Healthy Young Adults

Michael Rosario, Andres Velez Lopez, Rachel Nauer, Karin Schon

Brain Plasticity and Neuroimaging Lab, Boston University School of Medicine, Boston, MA 02118

Background: Studies using rodent models have shown a positive correlation between voluntary wheel running and neuroplasticity and neurogenesis in the medial temporal lobes (MTL), especially in the hippocampus (HC). The MTL include not only the HC, but also the entorhinal cortex (EC), among other regions, which serves as a primary input to the HC formation. Both are brain areas that are well-known to be critical for memory formation and that show early pathology in Alzheimer's disease. In order to test whether these rodent models could translate to humans, our lab previously used a voxel-based volumetric analysis to assess a relation between EC volume, cardiovascular fitness (VO2 max), and recognition memory in a cohort of healthy young human adults. This previous analysis showed right EC volume, but not HC volume was positively correlated with VO2 max. Here, using a surface-based analysis in a new young human cohort, we hypothesized that VO2 max would be positively correlated with EC thickness and with performance on tests of spatial cognition that are known to recruit the EC in healthy young adults.

Methods: We conducted an exploratory brain analysis using Freesurfer for a cross-sectional, surface-based analysis of cortical thickness, an analysis of subcortical volumes, and regions of interest analysis of the HC and EC. These outcomes were used for a multiple regression analysis using VO2 max and measures of spatial cognition as predictors in a cohort of 25 healthy young adults (ages 18-35). We determined VO2 max using a modified-Balke protocol treadmill test. We used age, gender, and intracranial volume as covariates.

Results: A multiple regression analysis significantly predicted left EC thickness using VO2 max (F (4, 20) = 4.58, p < .01, r^2 = 0.37), holding age, gender, and intracranial volume constant. Greater VO2 max and age were independently associated with greater left EC thickness (r = 0.495 , p < 0.01, r = 0.388, p < 0.05, respectively). No significant relationships were identified for measures of spatial cognition with EC thickness or VO2 max.

Conclusions: Consistent with our hypothesis and our previous work with human participants, VO2 max was positively correlated with left EC thickness. This data further support that cardiovascular fitness may be implicated in the plasticity of structures in the MTL, even in healthy young adults. Our cross-sectional data suggest aerobic exercise should affect plasticity of MTL structures in the healthy human brain, which is the current research focus in the Brain Plasticity and Neuroimaging Lab.

Logan Wolfel
New Mexico Highlands University
Class of 2018

Differentiation of Embryonic Stem Cells to Thyroid Lineages

Logan Wolfel, Keri Dame, Matt Lawton, Laertis Oikonomou

Center for Regenerative Medicine, Boston University School of Medicine, Boston Medical Center, Boston, MA 02118

Background: Thyroid related disorders are a prominent issue in modern American culture. This issue has led to research in directed differentiation of pluripotent stem cells into functional thyroid follicles. Through manipulation of signaling pathways during the different developmental stages, mouse embryonic stem cells (mESCs) are directed toward a thyroid lineage. Indicative of this differentiation stage is the transcription factor Nkx2-1, which is expressed in the developing forebrain, lung and thyroid. This system will serve as a model for future in vitro development of functional thyroid cells from human iPS cells.

Methods: An inducible Nkx2-1 transgene was previously introduced to a line of mESCs using the Cre-LoxP recombination system. Two clones of this line were then run through a directed differentiation protocol to test for induction efficiency of the thyroid lineage. The two clones were interrogated using immunostaining for proteins of interest as wells as analyzed through flow cytometry to quantify the expression of the transgene. Lentiviral transduction of FG-293 cells was also preformed to test the expression of a transgene containing Nkx2-1 and a reported fluorophore. Finally the rat thyrocyte FRTL5 line was used to optimize the iodine uptake functional assay.

Results: The two untested clones taken from the inducible line had their transgene induction efficiency compared to a line with a high transgene expression of 90-95%. Upon flow cytometry analysis, the first clone produced 29% Nkx2-1 positive cells while the second produced 67%. Falling short of the 90-95% goal, these differentiations were discontinued at day five of the protocol and additional clones will be tested. Likewise, the viral integration also proved troublesome. The mechanism utilized an inducible system which directs two viruses to integrate two gene constructs into a host cell, Nkx2-1-GFP and rtTA. This system then takes advantage of the Tet-on system in which doxycycline is required to facilitate rtTA binding and transcription of Nkx2-1, which ultimately produces GFP fluorescence. However, these cells expressed varied amounts of GFP regardless of doxycycline and rtTA concentrations. Conversely, promise was shown by the immunostaining protocols. We stained mESC derived developmental intermediated and matured thyroid progeny to test for marker protein expression levels. For both conjugated and unconjugated versions of Ki-67 fluorescence was observed, indicating active proliferation. The day 30 thyroid follicles stained with Nkx2-1 and the thyroid marker Pax8 also exhibited notable amounts of fluorescence. In the case of the iodine uptake assay FRTL5 cells were cultured in a variety of substrates which helped optimize the protocol.

Conclusion: The transgene inducible system requires additional clone testing to find a line that provides a high yield of Nkx2-1 while the iodine uptake requires increased variable testing to optimize the assay. The inconsistent results of the transgene induction in the FG293 cells will be addressed by using a mESC line that usually shows a lesser degree of transgene leakiness.

Boston University Graduate Medical Sciences

Summer Training as Research Scholars

The STaRS program would like to acknowledge the achievements of our students and the faculty and researchers across BU Medical Campus whose mentorship has enhanced both the quality of our students' work and their overall summer experience. Thank you!

Name	Home Institution	Mentor
Chioma Anyikwa	Boston University School of Medicine	Francesca Seta, PhD
Marissa Baccas	Fayetteville State University	Isabel Dominguez, PhD
Erika Banuelos	Brown University	Jiyoun Kim, PhD
Denston Carey	West Chester University of Pennsylvania	Jennie Luebke, PhD
Nirisha Commodore	University of the Virgin Islands	David Sherr, PhD
Kevin Delijani	Emory University	Lee Wetzler, MD
Celina Duran	Boston University School of Medicine	Renda Weiner, MD
Yuying Guo	Bryn Mawr College	John H Connor, PhD
Chino Igwebuike	Boston University School of Medicine	Steven Borkan, MD
Jabari Jackson	Tougaloo College	Angela Havasi, MD
Charles Laurore	Williams College	Matt Layne, PhD
Kathryn Odamah	Duke University	Feng Hui, MD PhD
Joanna Ortega	Boston University School of Medicine	Andrew Wilson, MD
Luis Perez Valencia	Connecticut College	Debbie Stearns-Kurosawa, PhD
Tyler Pluchino	Upstate Medical University, SUNY	Rick Ruberg, MD
Lauren Roberts	Boston University School of Medicine	Jeffrey Siracuse, MD
Kyle Rodrigues	University of Massachusetts, Amherst	Richard Wainford, PhD
Michael Rosario	University of the Virgin Islands	Karin Schon, PhD
Logan Wolfel	New Mexico Highlands University	Laertis Oikonomou, PhD